Available online at www.sciencedirect.com
ScienceDirect
Journal of Solid State Chemistry 181 (2008) 450–456
JOURNAL OF SOLID STATE CHEMISTRY
www.elsevier.com/locate/jssc

# Novel three-dimensional dandelion-like $TiO_2$ structure with high photocatalytic activity

Xuelian Bai, Bin Xie, Nan Pan, Xiaoping Wang, Haiqian Wang*

*Hefei National Laboratory for Physical Sciences at Microscale, University of Science and Technology of China, 96 Jinzhai Road, Hefei, 230026 Anhui, People's Republic of China*

Received 10 August 2007; received in revised form 23 November 2007; accepted 16 December 2007
Available online 25 December 2007

**Abstract**

Pure rutile phase crystalline $TiO_2$ powder with novel 3D dandelion-like structure was synthesized by using a facile hydrothermal method with $TiCl_3$ as the main starting material. In such a 3D structure, the nanometer-scale construction elements aggregate together and form a micrometer-scale artificial unit. The typical 3D dandelion structure has an average diameter of 1.5–2 μm and is packed radially by nanorods with [001] preference growth direction. Each individual nanorod is hundreds of nanometers in length, and tens of nanometers in diameter. The obtained 3D dandelion-like $TiO_2$ powder has a high photocatalytic activity, which is equivalent to that of the commercial available P25 titania powder. Mechanisms of the formation of the dandelion-like structure were also discussed. A different oxidation process of Ti(III) to Ti(IV) during hydrothermal was suggested.


*Keywords:* Titania; 3D structure; Hierarchical structure; Hydrothermal; Photocatalytic activity

## 1. Introduction

Titania ($TiO_2$), a semiconductor with a direct bandgap of 3.2 eV, exhibits a wide range of potential technological applications, including photocatalysis of pollutants [1,2], photosplitting of water [3], transparent conducting electrodes for dye-sensitized solar cells [4–6], etc. It becomes more and more evident that, besides the chemical composition, scaling down a material to the nanometer-scale range while keeping the dimensionality, size, and crystal structure under well control may bring some novel and unexpected properties [7,8]. Apart from nanoparticles [9], nanorods [10], nanowires [11], and nanotubes [12,13], three-dimensional (3D) titania hierarchical structures with hollow spheres [14,15] and glomerate spheres were reported recently [16–22]. For example, Wu et al. [16] synthesized titania nanoflowers by oxidizing pure titanium with hydrogen peroxide solutions at low temperature, an excellent photocatalytic performance was demonstrated. By hydrothermal treatment of titanium trichloride/NaCl solution, Fujihara and co-workers [20] and Jiang and co-workers [21] synthesized 3D titania hierarchical structure films on glass substrate with nanorods arranged radially. Reversible superhydrophobicity/superhydrophilicity was observed in such films [21]. In such a 3D structure, the nanometer-scale construction elements aggregate together and form a micrometer-scale artificial unit. This kind of 3D artificial hierarchical titania structure has the advantage of reserving the novel nanometer-scale properties (e.g., high photocatalytic activity) while providing us the convenience of storing and handling as we routinely enjoyed for the micrometer-scale materials [23]. For example, when used as a photocatalyst, 3D microscale titania powder has less aggregation and is easy to be separated from the solution as compared to nanometer-scale powders. Therefore, it is of great scientific and industrial importance to explore novel 3D titania structures and find economical mass production methods which can keep the morphology of the 3D hierarchical titania under effective control.

Herein, $TiO_2$ powders with novel 3D dandelion-like structures were synthesized by using a facile hydrothermal method, which is easy to be scaled up to mass production capability. The influences of various experimental parameters,

*Corresponding author. Fax: +86 551 3606266.
*E-mail address:* hqwang@ustc.edu.cn (H. Wang).

0022-4596/$ - see front matter © 2007 Elsevier Inc. All rights reserved.
doi:10.1016/j.jssc.2007.12.019

including the reaction time, reaction temperature, reactants concentration, and the pH value of the original solution, on the morphology of the 3D $TiO_2$ structure were studied. The obtained 3D dandelion-like $TiO_2$ powder reveals a high photocatalytic activity, which is equivalent to that of the commercial available P25 titania powder [24,25].

## 2. Experimental

### 2.1. Sample preparation

The 3D $TiO_2$ structures were synthesized via hydrothermal method. The starting material, titania(III) chloride–hydrochloride acid solution which contains 15 wt% of $TiCl_3$, was dissolved in water, and then supersaturated NaCl with 99.5 wt% purity was added. In some of the experiments, NaOH of 96 wt% purity was used to control the pH value of the solution. After stirring for 10 min at room temperature, 15 mL of the aqueous solution was transferred to a 20-mL Teflon-lined stainless steel autoclave reactor. The autoclave was put into an electric oven. Then, the oven was heated to the reaction temperature (typically 190 °C) and kept for a specific period of time (typically 240 min). After cooling down, the products were collected through centrifugation, washed five times with deionized water and three times with pure ethanol. After drying at room temperature overnight, the obtained $TiO_2$ powder was ready to be used.

### 2.2. Sample characterizations

The morphology and microstructure of the $TiO_2$ powders were analyzed directly by field-emission scan electron microscopy (FE-SEM; JEOL-JSM-6700F), X-ray diffraction (XRD; MXPAHF), and high-resolution transmission electron microscopy (HRTEM), respectively.

### 2.3. Photocatalytic reaction

The photocatalytic activity of the dandelion-like $TiO_2$ powder was examined by the degradation of methyl orange (MO) under UV light illumination. Thirty milliliters of $3 \times 10^{-3}$ mol/L MO solution was employed as a target, and 0.03 g $TiO_2$ powder was added into the MO solution as catalyst. The mixture was sealed inside a 50-mL-volume quartz vessel and dispersed by stirring for 30 min in dark. A 400-W high-pressure mercury lamp fixed at a distance of 8 cm above the surface of the solution was used as UV light source. Then, the degradation reaction was performed by stirring the suspension under light irradiation while keeping the temperature at 20 °C with a cooling water bath. The $TiO_2$ catalyst was removed from the degraded MO solution by centrifugation before the absorption spectra were taken by a UV–vis–IR spectrometer (Hitachi U4100).

## 3. Results and discussion

### 3.1. Structure and morphology

Fig. 1a shows a typical SEM image of the $TiO_2$ powder, which was obtained by heating the $[TiCl_3] = 0.09$ M, $[NaCl] = 10$ M and $pH = 3$ solution at 190 °C for 240 min. Here, $[TiCl_3]$ and [NaCl] represent the concentrations of $TiCl_3$ and NaCl, respectively. The inset in Fig. 1a shows an enlarged individual dandelion-like $TiO_2$ sphere. The overall 3D structure appears to be elegant spheres with an average diameter of about 1.5–2 μm. By a close examination of the top surface (Fig. 1b), we can see that the sphere was composed of many loosely packed nanometer-scale crystals with square-shaped ends. The crashed section of a sphere (Fig. 1c) reveals that it was packed with many nanorods radially. This kind of 3D titania sphere structure will be called as "dandelion-like structure" in the following text, in analog with the plants of the same name in the nature. In a dandelion, the diameters of the nanorods are about 15 nm, and the lengths are in the hundreds of nanometers scale. Fig. 2a gives the HRTEM image of a nanorod viewed from the sidewall direction as indicated in the inset. The distance between the adjacent lattice fringes (0.325 nm) can be assigned to the interplanar distance of rutile $TiO_2$ (1 1 0). The nanorods have therefore grown along the [001] axis. The corresponding SAED pattern in Fig. 2b displays the single-crystalline nature and could be indexed to the pure rutile $TiO_2$ phase. The XRD pattern of the $TiO_2$ powder is shown in Fig. 3. All of the reflection peaks can be readily indexed to pure rutile $TiO_2$. No characteristic peak was detected for impurities. The sharpness of the peaks implies a high crystallinity of the $TiO_2$ products.

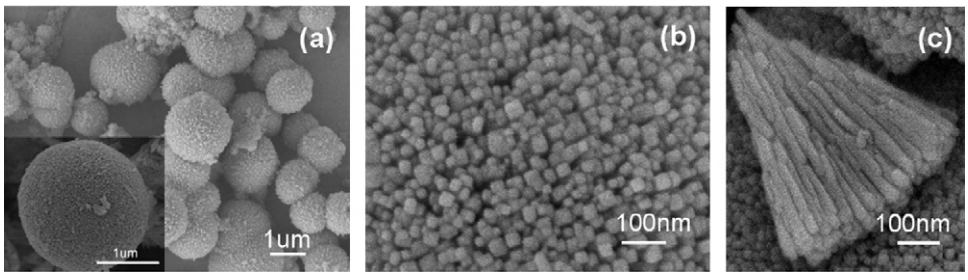


Fig. 1. (a) SEM image of the $TiO_2$ powder. *Inset*: an enlarged individual dandelion-like $TiO_2$ sphere. (b) Top image of a dandelion. (c) Crash section of a dandelion.

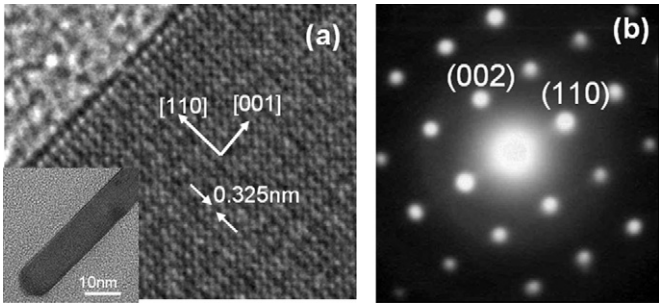


Fig. 2. (a) HRTEM and the TEM (inset) images of an individual nanorod and (b) SAED pattern of part (a).

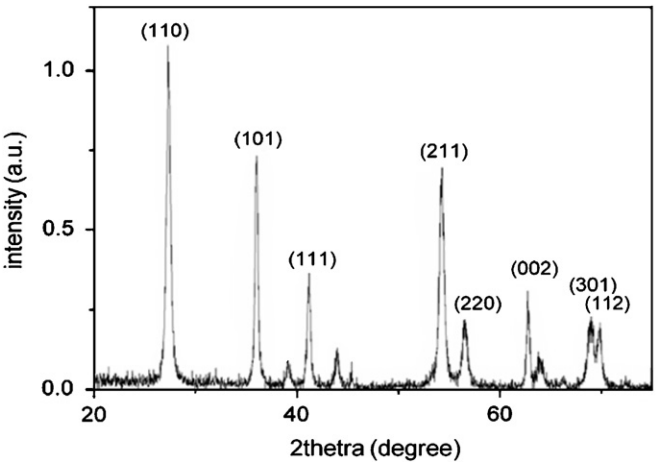


Fig. 3. XRD of the $TiO_2$ powder.

### 3.2. Effects of synthesis parameters on the morphology and crystal phase of $TiO_2$

In the following context of this section, we will demonstrate that the morphology and crystal phase of the 3D $TiO_2$ hierarchical structures can be tuned by controlling the reaction time, reaction temperature, reactant concentrations, as well as the solution's pH value.

#### 3.2.1. Effect of reaction time

To investigate the morphological evolution of the dandelion $TiO_2$, the $[TiCl_3] = 0.09$ M, $[NaCl] = 10$ M and $pH = 3$ solution was heated at 190 °C for various reaction times. The morphology evolution of the products with the reaction time is illustrated in Fig. 4. When the reaction time was short (e.g., 1 min, as shown in Fig. 4a), only aggregated nanoparticles were observed in the products, the average diameter of the nanoparticles was about 40 nm. Prolonging the reaction time to 60 min, aggregated nanorods can be observed (Fig. 4b). When the reaction time reaches 120 min, dandelion-like structures with an average diameter of about 0.7 μm were formed (Fig. 4c). Further extending the reaction time to 240 min, the dandelions became more round in shape and the nanorods were packed more closely. Meanwhile, the average diameter of the dandelions also grew to about 1.5 μm (Fig. 4d).

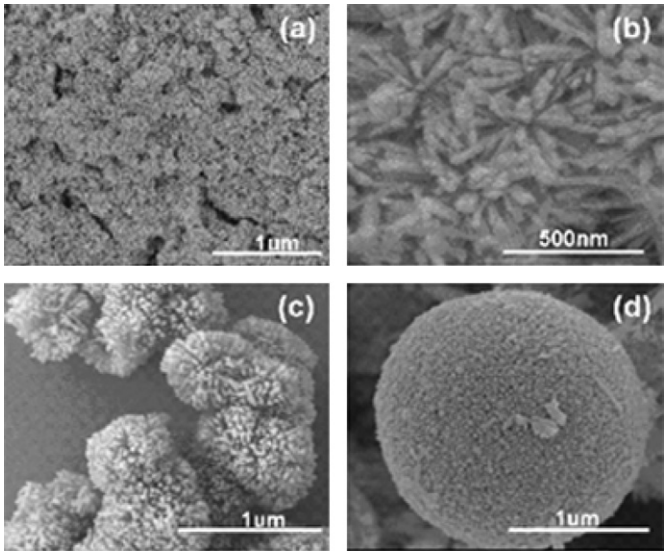


Fig. 4. SEM images of nanostructures obtained at different times: (a) 1 min, (b) 60 min, (c) 120 min, and (d) 240 min.

#### 3.2.2. Effect of temperatures

In Fig. 5, dandelions obtained from the $[TiCl_3] = 0.09$ M, $[NaCl] = 10$ M and $pH = 3$ solution heated for 240 min at different temperatures are illustrated. At 160 °C reaction temperature, the dandelions were formed by loosely packed nanorods, and the lateral size of the nanorods was distributed in a wide range from 10 to about 50 nm. The ends of the nanorods are square in shape, indicating that the titania is in the rutile phase, which is consistent with our XRD results. Raising the reaction temperature to 180 and 190 °C, the obtained dandelions became more and more compact, while the size of the nanorods reduces. At lower temperatures, the hydrolysis reaction takes place in a more equilibrium environment, so the nanorods may grow larger. In the inspected reaction temperature range, the overall diameter of the dandelions had no obvious change.

#### 3.2.3. Effect of NaCl concentration

Fig. 6 shows the morphology changes of the 3D $TiO_2$ hierarchical structure with NaCl concentration. The experiment was performed on a solution of $[TiCl_3] = 0.09$ M and $pH = 3$. The reaction temperature was 190 °C and the reaction time was 240 min. Without any NaCl addition, only small dandelions with sizes of about 300 nm were observed. Increasing [NaCl] from 7 to 11 M, the size of the dandelions increases from hundreds of nanometers to a few micrometers. The packing density of the dandelions also increases with the NaCl concentration. XRD patterns show that all the samples were pure rutile $TiO_2$. The roles of NaCl in the formation of the 3D structure were considered to be (1) retarding the formation of $TiO_2$ grow in the [110] direction and (2) promoting the $TiO_2$ nanorods grow in the [001] direction [20].

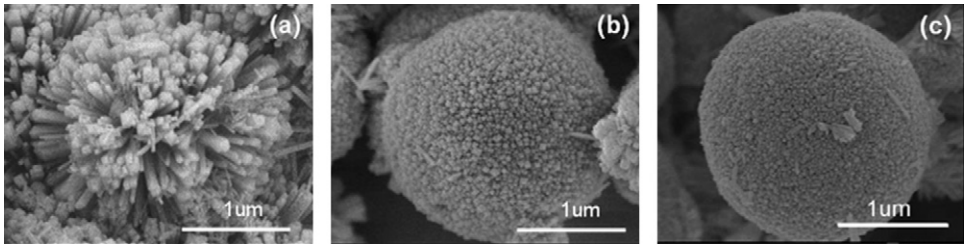


Fig. 5. SEM images of nanostructures obtained at different temperatures: (a) 160 °C, (b) 180 °C, and (c) 190 °C.

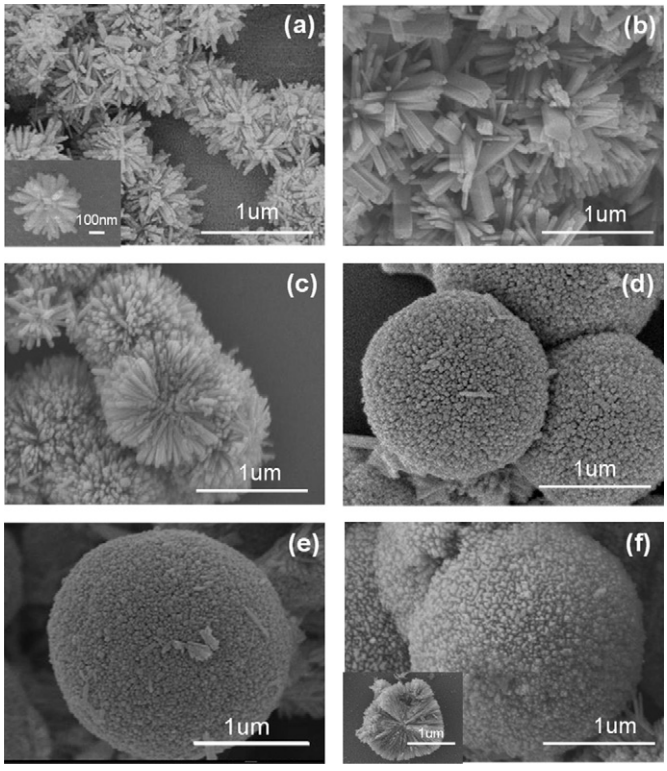


Fig. 6. SEM images of the synthesized $TiO_2$: (a) [NaCl] = 0 M, (b) [NaCl] = 7 M, (c) [NaCl] = 8 M, (d) [NaCl] = 9 M, (e) [NaCl] = 10 M, and (f) [NaCl] = 11 M.

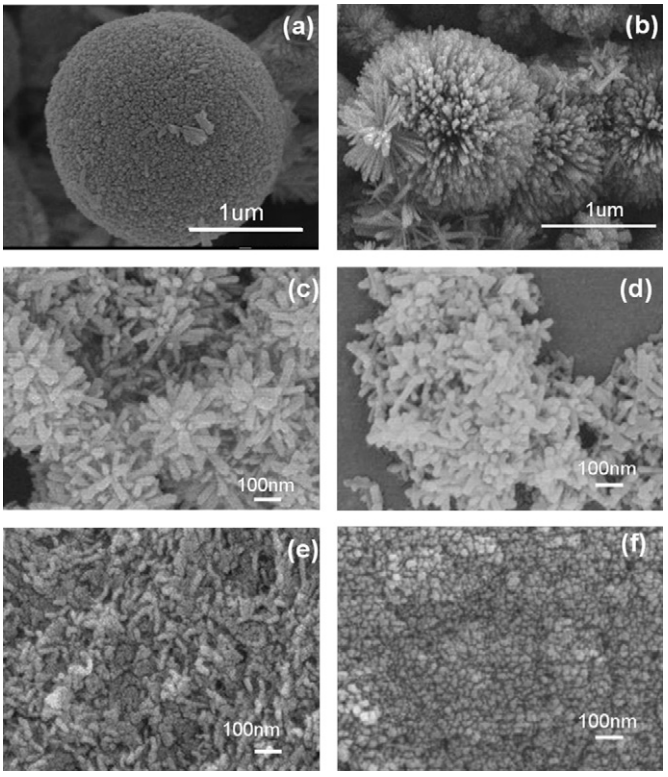


Fig. 7. SEM images of nanostructures obtained at different pH values: (a) pH = 3, (b) pH = 4, (c) pH = 5, (d) pH = 7, (e) pH = 10, and (f) pH = 13.

### 3.2.4. *Effect of pH*

The original pH value of the $[TiCl_3] = 0.09$ M, and [NaCl] = 10 M solution is 3. The pH value of the solution was adjusted by adding NaOH into the original solution. Then, the solution was thermally treated at 190 °C for 240 min. Fig. 7 displays the products obtained with solutions of different pH values. The size and packing density of the dandelions became smaller and smaller when the pH value changes from 3 to 5. Further increasing the pH value to over 7, only irregular nanorods remain, no dandelion structure can be observed any longer. When the solution become highly alkaline (pH = 13), only nanoparticles of about 15 nm in diameter can be obtained. Overall, increasing the pH value destroys the 3D dandelion structure.

Fig. 8 shows the XRD patterns of $TiO_2$ samples obtained from the solutions of pH = 3–13. Only pure rutile phase (major peaks at 27.44°, 36.01°, 54.32°) were detected for the pH = 3, 4, and 5 samples. When the solution's pH value was increased to 7, anatase phase (major peaks at 25.30°, 37.80°, 48.14°) emerges. For the pH = 10 sample, highly crystalline anatase phase was observed. For titania mixture with anatase and rutile phases, the mass fraction of rutile phase can be estimated using the following formula [26]:

$$R\% = 1 - \left[1 + 1.26\left(\frac{I_R}{I_A}\right)\right] - 1,$$

where $I_R$ and $I_A$ are the X-ray-integrated intensities of the rutile (1 1 0) diffraction peak and the anatase (1 0 1) diffraction peak, respectively. Therefore, the fraction of the rutile phase in the pH = 7 and 10 samples was estimated to be 91.7 and 15 wt%, respectively. While for the pH = 13 sample, only pure anatase phase $TiO_2$

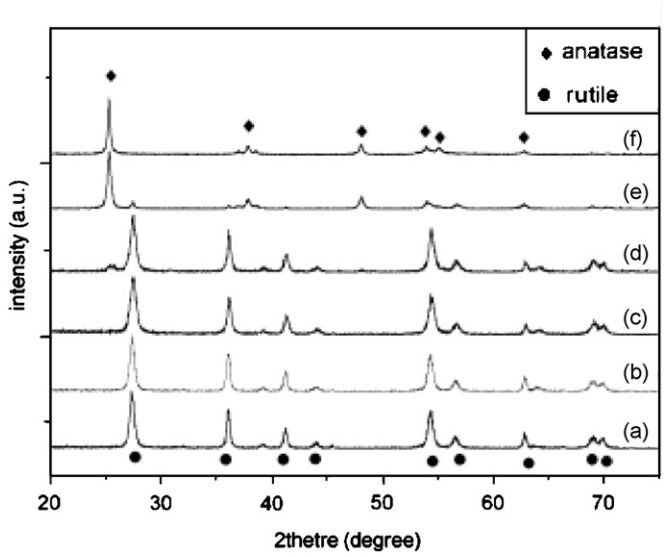


Fig. 8. XRD patterns of $TiO_2$ obtained from starting solutions with different pH values: (a) pH = 3, (b) pH = 4, (c) pH = 5, (d) pH = 7, (e) pH = 10, and (f) pH = 13. (◆): Anatase, (●): Rutile.

structure was observed. The phenomenon that an acidic environment favors the formation of the rutile phase was also reported by Zhu et al. [27].

### 3.3. Discussions

The time evolution of the titania growth (Fig. 4) indicates a three-step growth process. At the very beginning, $TiO_2$ nanoparticles were precipitated in the solution as a result of homogeneous nucleation [20]. As the reaction time proceeds, aggregated nanorods (loosely packed immature dandelions) and densely packed mature dandelions with the [001] preference nanorods growth direction were formed succeedingly. We think that a nucleation and growth mechanism is responsible for the formation of the dandelion structure. By inspecting Fig. 1c and Fig. 4b and c, we can see that the nanorods, which can form the mature dandelions (Fig. 4d), are not uniform and continuous along the entire radius of the dandelions. On the contrast, the well-crystallized nanorods, which happened at lower reaction temperature (Fig. 5) or lower NaCl concentration (Fig. 6), can only form the loosely packed immature dandelions. This suggests that in the nucleation and growth process, some newly nucleated nanorods, which grow along the radial direction and misaligned with respect to the originally aggregated nanorods, promote the growth of the densely packed mature dandelions. The driving force for the nanorods growing in the radial direction should be the space-limited crystallization. A similar rutile-phase $TiO_2$ 3D dandelion-like structure with [101] preference nanorod direction was observed by Liu et al. [28] by performing thermohydrolysis of $TiCl_3$ aqueous solution with the addition of urea and surfactant, and the authors suggested a three-step nucleation and growth mechanism.

However, as we can see from Fig. 4, the number of nanoparticles and immature dandelions are far more than the number of the mature dandelions. Therefore, in addition to the nucleation and growth mechanism, there must also be another mechanism that is responsible for the mass transportation of titanium cations from one $TiO_2$-aggregated structure to another one.

From the experimental results of Fig. 7, we can see that the pH value of the original solution has an important effect on the morphology of the final products. The first explicit effect of pH value on the final product is through the following reaction equation [20]:

$$Ti^{3+} + H_2O \rightarrow TiOH^{2+} + H^+ \quad (1)$$

In a highly acidic solution, the high concentration of $H^+$ cations restrains the hydrolysis and results in a low reaction rate. A low reaction rate favors the agglomeration of $TiO_2$ particles [29,30] and the formation of 1D nanorods via heterogeneous nucleation. Moreover, we think that the solubility of $TiO_2$ in the high concentrated HCl solution should be the reason for the mass transportation between the aggregated $TiO_2$ structures. Under proper experimental conditions, once a dandelion is formed through the nucleation and growth mechanism, it will have a lower surface energy as compared to nanoparticles and nanorods. The solubility of $TiO_2$ in the HCl solution keeps a dynamic equilibrium between the immature aggregated solid $TiO_2$ structures (e.g., nanoparticles and nanorods) and the concentration of titanium cations in the solution. As a result of mass transportation mediated by the solution, the nanoparticles or the immature $TiO_2$ structures with high surface energies will disappear while the stable mature dandelions will grow up. The solubility of $TiO_2$ decreases with the decrease of HCl concentration in the solution, this also explains why we cannot obtain large 3D structures in solutions with high pH values (see Fig. 7).

As discussed earlier, the high NaCl concentration and small pH value favor the formation of the dandelions. The $Cl^-$ and $H^+$ ions both suppress the hydrolysis reaction due to the common ion effect. The $Cl^-$ ions also selectively suppress the growths on {1 1 0} crystalline surfaces of $TiO_2$, and therefore promote the nanorods growth along the [001] direction [20]. On the other hand, the $H^+$ ions may change the surface charge properties of $TiO_2$ [31], and in turn dramatically change the aggregation state of the $TiO_2$ products.

Regarding the oxidation of the trivalence $Ti^{3+}$ cations in the starting solution to the tetravalence $Ti^{4+}$ in the final $TiO_2$ product, Fujihara and co-workers [20] suggested that the dissolved oxygen in the original solution acts as the oxidant. However, in our experiments, it is easy to estimate that there is not enough oxygen (including the dissolved oxygen and the oxygen sealed inside the autoclave) to oxidize the $Ti^{3+}$ to reach the final ~90 mol% yield of $TiO_2$. So, we analyzed the residual gas sampled from the autoclave after the synthesis reaction finished by a gas chromatograph (GC-14C, Shimadza). After the autoclave

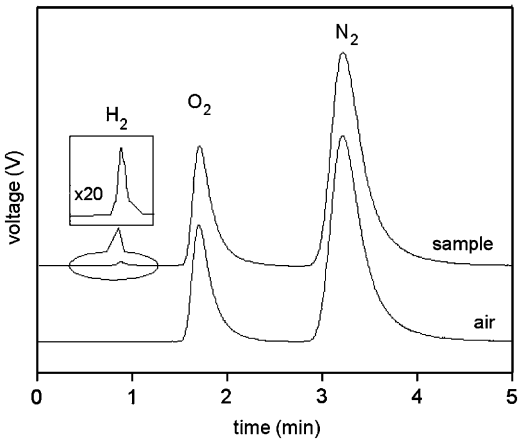


Fig. 9. Residual gas composition analyzed by a gas chromatograph.

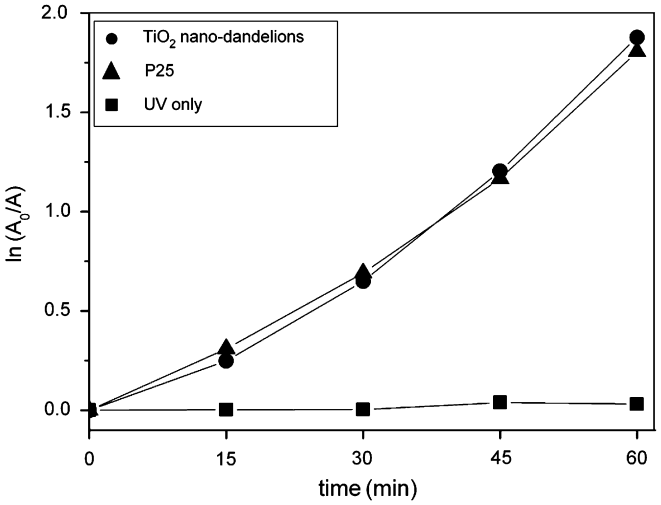


Fig. 10. Photodegradation of MO in water catalyzed by (●) the $TiO_2$ powder with 3D dandelion-like structure as shown in Fig. 1a and (▲) the P25 powder, (■) applying UV radiation only (without addition of any kind of $TiO_2$). The initial composition of the solution is $[MO_0] = 3 \times 10^{-3}$ mol/L and the catalyst concentration is 1 g/L.

was cooled down to room temperature, it was sealed inside a rubber bag. Then, we opened the autoclave and sampled the residual gas with an injector. Because we cannot remove the air inside the rubber bag thoroughly, so the $O_2$ and $N_2$ signals were very strong. Even so, it can be seen from Fig. 9 that a $H_2$ signal peak was clearly resolved. As a comparison, only $O_2$ and $N_2$ signal peaks were detected from the air sample. Based on these facts, we would like to suggest that, at the very beginning, the oxidation process can be a reaction with dissolved oxygen, as suggested by Fujihara and co-workers [20]:

$$TiOH^{2+} + O_2 \rightarrow \text{Ti(IV) oxo species} + O_2^- \rightarrow TiO_2 \quad (2)$$

After the dissolved oxygen was exhausted, the following oxidation process becomes dominant:

$$Ti(III)OH^{2+} + H^+ \rightarrow \text{Ti(IV) oxo species} + H_2 \rightarrow TiO_2 \quad (3)$$

Undoubtedly, reaction (3) is not as energetically favorable as reaction (2). Nevertheless, the catalytic behavior of the previously formed titania, the high reaction temperature and pressure may all promote reaction (3) to the right direction.

### 3.4. Photodegradation

Fig. 10 compares the photocatalytic activity of the 3D dandelion-like $TiO_2$ powder (Fig. 1a) with the commercial P25 $TiO_2$ powder (Degussa). In Fig. 10, $A_0$ and $A$ are the absorptions corresponding to the 465-nm absorption peak of the MO solution before the photocatalytic reaction and at reaction time $t$, respectively. For an MO aqueous solution with a dilute initial concentration, the absorption $A$ is proportional to the MO concentration [32]. Therefore, $\ln(A_0/A) = \ln([MO_0]/[MO])$, where $[MO_0]$ and [MO] are the MO concentrations before and after the photocatalytic reaction, respectively. So, we know from Fig. 10 that the 3D dandelion-like $TiO_2$ powder obtained in this work has an equivalent photocatalytic activity with the commercial P25 $TiO_2$ powder. From Fig. 10, we can also see that by applying UV radiation only (without the addition of any $TiO_2$ catalyst), the MO concentration remains almost unchanged. This assures that the change of [MO] comes from the photocatalytic effect of the $TiO_2$ powders.

The commercial P25 powder is an optimized $TiO_2$ product with mixed rutile and anatase phases. Ohno and co-workers [33] reported that a mixed phase consisting of rutile and anatase types of $TiO_2$ has a higher photocatalytic activity than the pure anatase or pure rutile $TiO_2$. In a previous work, Wu et al. [16] synthesized mixed-phase titania nanoflowers which exhibited nearly the same photocatalytic activity as that of P25. Xie et al. [15] reported that rutile-phase $TiO_2$ hollow spheres exhibited superior photocatalytic activities over $TiO_2$ nanorods but somewhat poorer than P25. In this work, the photocatalytic activity of the 3D dandelion-like $TiO_2$ powder is equivalent to that of the P25 $TiO_2$ powder; even the dandelions are in the pure rutile phase. Although we cannot understand the detailed underlying mechanism of the high photocatalytic activity at the present time, we believe that the well-controlled 3D hierarchical structure should be an important factor.

## 4. Conclusions

Pure rutile phase $TiO_2$ powders with novel 3D dandelion-like structures were synthesized by using a facile hydrothermal method with $TiCl_3$ as the main starting material. The 3D dandelion structure has an average diameter of 1.5–2 μm and is packed radially by nanorods with a [001] preference growth direction. Each individual nanorod is hundreds of nanometers in length, and tens of nanometers in diameter. A three-step nucleation and growth mechanism of nanoparticles, aggregated nanorods,

and 3D dandelion-like structure was confirmed. Mass transportation of titanium cations between the aggregated $TiO_2$ structures was discussed. A new oxidation process of Ti(III) to Ti(IV) was proposed. The obtained 3D dandelion-like $TiO_2$ powder has a high photocatalytic activity, which is equivalent to that of the commercial available P25 titania powder.

## Acknowledgments

This work is supported by the National Natural Science Foundation of China (50121202, 90406009), National Research Foundation for the Doctoral Program of the Ministry of Education under grant 20040358059 and National Basic Research Program of China (2006CB922002).

## References

[1] T.B. Ghosha, S. Dhabal, A.K. Datta, J. Appl. Phys. 94 (2003) 4577–4582.
[2] M. Sixto, B. Julian, V. Alfonso, R. Christoph, Appl. Catal. B 37 (2002) 1–15.
[3] J.H. Park, S. Kim, A.J. Bard, Nano Lett. 6 (2006) 24–28.
[4] M. Gratzel, Nature 414 (2001) 338–344.
[5] K.J. Kim, K.D. Benksten, J.V.D. Lagemaat, A.J. Frank, Chem. Mater. 14 (2002) 1042–1047.
[6] N.G. Park, J.V.D. Lagemaat, A.J. Frank, J. Phys. Chem. B 104 (2000) 8989–8994.
[7] H.C. Zeng, J. Mater. Chem. 16 (2006) 649–662.
[8] P. Alivisatos, J. Phys. Chem. 100 (1996) 13226–13239.
[9] R. Alexandrescu, F. Dumitrache, I. Morjan, I. Sandu, M. Savoiul, I. Voicu, C. Fleaca, R. Piticescu, Nanotechnology 15 (2004) 537–545.
[10] H.M. Cheng, J.M. Ma, Z.G. Zhao, L.M. Qi, Chem. Mater. 7 (1995) 663–671.
[11] Z. Miao, D.S. Xu, J.H. Ouyang, G.L. Guo, X.S. Zhao, Y.Q. Tang, Nano Lett. 2 (2002) 717–720.
[12] G.Y. Guo, J.S. Hu, H.P. Liang, L.J. Wan, C.L. Bai, Adv. Funct. Mater. 15 (2005) 196–202.
[13] T. Kasuga, M. Hiramatsu, A. Hoson, T. Sekino, K. Niihara, Adv. Mater. 11 (1999) 1307–1311.
[14] H.G. Yang, H.C. Zeng, J. Phys. Chem. B 108 (2004) 3492–3495.
[15] X.X. Li, Y.J. Xiong, Z.Q. Li, Y. Xie, Inorg. Chem. 45 (2006) 3493–3495.
[16] J.M. Wu, B. Huang, M. Wang, A. Osaka, J. Am. Ceram. Soc. 89 (2006) 2660–2663.
[17] M.H. Huang, S. Mao, H. Feick, H. Yan, Y. Wu, H. Kind, E. Webber, R. Russo, P. Yang, Science 292 (2001) 1897–1899.
[18] C. Biel, B.J. Ravoo, D.N. Reinhoudta, J. Huskens, J. Mater. Chem. 16 (2006) 3997–4021.
[19] T.N. Hou, J. Li, M.K. Smith, P. Nguyen, A. Cassell, J. Han, M. Meyyappan, Science 300 (2003) 1249.
[20] E. Hosono, S. Fujihara, K. Kakiuchi, H. Imai, J. Am. Chem. Soc. 126 (2004) 7790–7791.
[21] X.J. Feng, J. Zhai, L. Jiang, Angew. Chem. Int. Ed. 44 (2005) 5115–5118.
[22] H. Xu, F.L. Jia, Z.H. Ai, L.Z. Zhang, Crystal Growth Des. 7 (2007) 1216–1240.
[23] S. Neeraj, S. Natarajan, Chem. Mater. 12 (2000) 2753–2762.
[24] J.L. Gole, J.D. Stout, C. Burda, Y. Lou, X. Chen, J. Phys. Chem. B 108 (2004) 1230–1240.
[25] J.M. Valtierra, J.G. Servia, C.F. Reyes, Y.S. Calixto, Rev. Mex. Ing. Quim. 4 (2005) 191–200.
[26] U. Balachandran, N.G. Eror, J. Solid State Chem. 42 (1982) 276–282.
[27] H.Y. Zhu, Y. Lan, X.P. Gao, S.P. Ringer, Z.F. Zheng, D.Y. Song, J.C. Zhao, J. Am. Chem. Soc. 127 (2005) 6730–6736.
[28] L. Liu, Y.P. Zhao, H.J. Liu, H.Z. Kou, Y.Q. Wang, Nanotechnology 17 (2006) 5046–5050.
[29] D.V. Bavykin, V.N. Parmon, A.A. Lapkina, F.C. Walsh., J. Mater. Chem. 14 (2004) 3370–3377.
[30] S. Yamabi, H. Imai, Chem. Mater. 14 (2002) 609–614.
[31] N. Guettaï, H.A. Amar, Desalination 185 (2005) 427–437.
[32] M.R. Hoffmann, S.T. Martin, W. Choi, D.W. Bahnemannt, Chem. Rev. 95 (1995) 69–96.
[33] J.G. Jia, T. Ohno, M. Matsumura, Chem. Lett. 29 (2000) 908–909.